Phase Transition Properties of 1-Alkyl- and 1-Acyl-2-amidophosphatidylcholines and Related Derivatives†

Babur Z. Chowdhry, Gert Lipka, Joseph Hajdu, and Julian M. Sturtevant*

ABSTRACT: The phase transition properties of aqueous dispersions of 1-alkyl- or 1-acyl-2-(*N*-acylamino)-2-deoxy-*sn*-glycero-3-phosphocholines and related 1-acyl-2-substituted phospholipids have been examined by high sensitivity differential scanning calorimetry. The phase transition properties of 1-*O*-octadecyl-2-(*N*-hexadecanoylamino)-2-deoxy-*sn*-glycero-3-phosphocholine (I) are most unusual for a pure lipid in showing a complex phase transition curve representable as the sum of five two-state transition components, a total calorimetric enthalpy of 27.9 kcal mol^{-1}, a temperature range of approximately 17 °C for the overall profile of apparent excess heat capacity vs. temperature, and, after sonication to produce small unilamellar vesicles, a complex phase transition curve, consisting of four two-state transition components. 1-*O*-Octadecanoyl-2-(*N*-octadecanoylamino)-2-deoxy-*sn*-glycero-3-phosphocholine (VI) shows a much simpler transition curve, the calorimetric parameters of which are similar to those of the corresponding saturated diacylphosphatidylcholine (distearoylphosphatidylcholine). The difference in phase transition properties between multilamellar vesicles of molecules I and VI arises in some unknown way from the existence in I of a 1-alkyl substituent compared to a 1-acyl substituent in VI. 1-*O*-Octadecyl-2-acetamido-2-deoxy-*sn*-glycero-3-phosphocholine (II) and 1-*O*-octadecyl-2-(2,2,2-trifluoroacetamido)-2-deoxy-*sn*-glycero-3-phosphocholine (III) give optically clear suspensions in doubly deionized water and, as expected from their chain lengths, do not exhibit any phase transitions in the temperature range −10 to 60 °C. 1-*O*-Octadecanoyl-2-[*N*-[(octyloxy)carbonyl]amino]-2-deoxy-*sn*-glycero-3-phosphocholine (IV) and 1-*O*-octadecanoyl-2-[*N*-[(octadecylamino)carbonyl]amino]-2-deoxy-*sn*-glycero-3-phosphocholine (V) also exhibit asymmetric curves of apparent excess heat capacity vs. temperature which can be analyzed into two-state component curves.

Alkyl and alk-1-enyl ether phospholipids occur in the membranes of both normal (Weber & Richter, 1982) and malignant mammalian cells (Howard et al., 1972) as well as in the membranes of halophilic bacteria (Kates, 1978). Ether-linked glycerophospholipids have been shown to be involved in a variety of physiological processes including platelet activation (Blank et al., 1981), vasodilation (Blank et al., 1979), and tumor cytotoxicity (Honma et al., 1981). Another class of phosphatidylcholine analogues, 1-acyl-2-deoxyamidophosphatidylcholines, are potent inhibitors of phospholipase activity (Bonsen et al., 1972). Recently, a number of enzymically nonhydrolyzable isosteric 1-acyl- and 1-alkyl-2-(*N*-acylamino)-2-deoxy-*sn*-glycero-3-phosphocholines and related 1-acyl-2- and 1-alkyl-2-substituted phospholipids of high purity have been synthesized (Chandrakumar & Hajdu, 1982, 1983). In view of the biological significance of lipids of these types, it is of interest to compare their physical and chemical properties with those of other types of phospholipids. In this paper we report the application of high sensitivity differential scanning calorimetry (DSC;[1] Mabrey & Sturtevant, 1978; Mabrey-Gaud, 1981) to the study of the phase transitions of the six phospholipids shown in Figure 1.

Although studies of the phase transition properties of certain phospholipids containing ether groups have been previously reported (Vaughan & Keough, 1974; Schwarz & Paltauf, 1977; Blume, 1976; Turcotte et al., 1977; Harlos et al., 1979; Sunder et al., 1978; Lee & Fitzgerald, 1980; Bittman et al., 1981; Boggs et al., 1981; Goldfine et al., 1981), comparable data for 2-(*N*-acylamino)-2-deoxy-*sn*-glycero-3-phosphocholines are not currently available.

Materials and Methods

Phospholipids. Stereospecific syntheses of compounds I–VI were conducted as previously reported (Chandrakumar & Hajdu, 1982, 1983). Elemental composition, infrared, proton magnetic resonance, and mass spectroscopic data were consistent with the structures given in Figure 1. The purity of all compounds was checked by TLC. The phospholipids (0.05 mg/10 μL) dissolved in chloroform exhibited single spots on Whatman K6F plates developed in chloroform/methanol/water (65:24:4 v/v/v) or chloroform/methanol/aqueous ammonia (1:9:1 v/v/v), the phospholipids being visualized by molybdic acid spray (Dittmer & Lester, 1964) and/or by iodine vapor. All other compounds used were of reagent grade except organic solvents which were of spectral grade.

Vesicle Preparation. Prior to vesicle preparation, the lipids were kept in a vacuum oven at 50 °C, until no further weight loss occurred. The lipids thus treated were in the form of dihydrates (Chandrakumar & Hajdu, 1983). Multilamellar liposomes (MLV's) were prepared by dispersing 1.0–5.0 mg in 2.0 mL of 0.01 M phosphate buffer (pH 7.0) in doubly deionized water or ethylene glycol/water mixtures (30% w/w).

† From the Department of Chemistry, Yale University, New Haven, Connecticut 06511 (B.Z.C., G.L., and J.M.S.), and the Department of Chemistry, Boston College, Chestnut Hill, Massachusetts 02167 (J.H.). *Received September 28, 1983.* This work was supported, in part, by grants from the National Institutes of Health (GM-04725) and the National Science Foundation (PCM78-24107) to J.M.S. and from the National Institutes of Health (AM 26165) to J.H.

[1] Abbreviations: PC, phosphocholine; I, 1-*O*-octadecyl-2-(*N*-hexadecanoylamino)-2-deoxy-*sn*-glycero-3-PC; II, 1-*O*-octadecyl-2-acetamido-2-deoxy-*sn*-glycero-3-PC; III, 1-*O*-octadecyl-2-(2,2,2-trifluoroacetamido)-2-deoxy-*sn*-glycero-3-PC; IV, 1-*O*-octadecanoyl-2-[*N*-[(octyloxy)carbonyl]amino]-2-deoxy-*sn*-glycero-PC; V, 1-*O*-octadecanoyl-2-[*N*-[(octadecylamino)carbonyl]amino]-2-deoxy-*sn*-glycero-3-PC; VI, 1-*O*-octadecanoyl-2-(*N*-octadecanoylamino)-2-deoxy-*sn*-glycero-3-PC; TLC, thin-layer chromatography; DSC, differential scanning calorimetry; *C* vs. *T*, curve of heat capacity vs. temperature; ΔH_{cal}, calorimetric enthalpy; $\Delta H'_{cal}$, total observed enthalpy for curve of *C* vs. *T*; ΔH_{vH}, van't Hoff enthalpy; C_{max}, maximal excess heat capacity; $T_{1/2}$, temperature of half-conversion; T_m, temperature at C_{max}; MLV's, multilamellar vesicles; SUV's, small unilamellar vesicles.

0006-2960/84/0423-2044$01.50/0

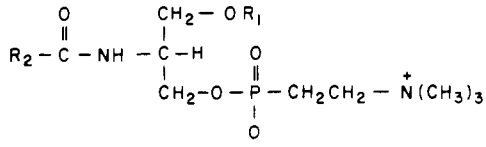

Compound	Substituent Groups	
	R_1	R_2
I	$(CH_2)_{17}CH_3$	$CH_3(CH_2)_{14}$
II	$(CH_2)_{17}CH_3$	CH_3
III	$(CH_2)_{17}CH_3$	CF_3
IV	$CO(CH_2)_{16}CH_3$	$CH_3(CH_2)_7O$
V	$CO(CH_2)_{16}CH_3$	$CH_3(CH_2)_{17}NH$
VI	$CO(CH_2)_{16}CH_3$	$CH_3(CH_2)_{16}$

FIGURE 1: Structural formulas of phospholipids[1] examined in this study.

Dispersion of compounds I and IV–VI was achieved by agitation on a vortex mixer for 40 s after heating to 10 °C above the highest phase transition temperature of each compound (approximate phase transition temperatures were found by heating from room temperature upward until dispersions were formed and by conducting some preliminary DSC experiments). This procedure was repeated 3 times. Electron micrographs (see below) showed these MLV's to have diameters of 7000–8000 Å and to be free of small vesicles. Compounds II and III were readily soluble in all solvents used at room temperature and gave solutions or suspensions with no visible turbidity.

Small Unilamellar Vesicles. SUV's of compound I were prepared by sonication of the lipid in doubly deionized water for 1 h under 1 atm of nitrogen at a temperature 10 °C above the highest temperature transition recorded for unsonicated lipid dispersions. A Branson ATH-610-10 sonication bath (Branson Instruments, Stamford, CT) was employed. After sonication the slightly turbid suspensions were centrifuged for 45 min by using a SW60 rotor in a Beckman L5-65 ultracentrifuge at $10^5 g$ to remove any multilamellar structures present and were then sonicated again for 10 min. After centrifugation suspensions with no visible turbidity were obtained.

Electron microscopy (see below) showed a homogeneous population of SUV's of 300–350-Å radius. To ensure that sonication had not produced any significant chemical changes, the lipid was extracted with $CHCl_3$, dried down under nitrogen and then in vacuo, resuspended in water, and rescanned in the calorimeter with no detectable change in transition properties from MLV's.

Extraction Methods. After calorimetry, a chloroform/methanol/water mixture (2:2:1 v/v/v) was added to 0.8 mL of lipid suspensions and the nonaqueous layer evaporated to dryness under nitrogen. Residual traces of organic solvent were removed by placing samples in vacuo overnight. The extracted compounds were analyzed by TLC after solution in chloroform (0.05 mg/10 μL) using the solvent systems given above, or they were resuspended in buffer and rerun in the calorimeter. Phosphorus was determined by published procedures (Dittmer & Wells, 1969; Stewart, 1980).

Calorimetry. DSC experiments were performed with a DASM-1M microcalorimeter (Privalov et al., 1975) using scan rates of 0.02–1.0 K min^{-1}. Instrumental base lines obtained by scanning buffer, doubly deionized water, or ethylene glycol/water mixtures in both sample and reference cells of the calorimeter were horizontal in the range 0–80 °C. The initial and final base lines for all curves of C vs. T were also horizontal with no significant changes in C. The noise level was in the range 0.01–0.02 kcal K^{-1} mol^{-1}. All samples were run in the calorimeter under a nitrogen pressure of 1.5 atm to minimize bubble formation. Subsequent to the DSC experiments, the lipids were extracted and examined by TLC. In no case was there any evidence of degradation.

Data Analysis. Transition curves were resolved into the sums of independent component curves which were required to follow the van't Hoff equation for a simple two-state process (Mabrey & Sturtevant, 1978). A computer program was employed that varied, in succession, the three parameters which characterize each van't Hoff curve until the standard deviation of the calculated sum curve from the observed data was minimal. A convenient set of parameters for each component curve is composed of the calorimetric enthalpy, ΔH_{cal}, proportional to the area of the transition curve, the van't Hoff enthalpy, ΔH_{vH}, which controls the variation with temperature of the equilibrium constant appropriate to the curve, and the temperature of half-conversion, $T_{1/2}$. The sum of the values for ΔH_{cal} for the resolved components agreed within a few percent with ΔH^t_{cal}, the total observed enthalpy evaluated by planimeter integration.

It should be emphasized that in the analysis of the data it has been assumed that any impurities are present in negligible amount. In the context of DSC experiments, the term negligible is considerably more restrictive than in other contexts. For example, the data for compound IV (Figure 5) can be fit with a single two-state curve having the parameters $T_{1/2}$ = 6.80 °C, ΔH_{cal} = 3.9 cal mol^{-1}, and ΔH_{vH} = 142 kcal mol^{-1} if it is assumed that a water-insoluble impurity is present at mole fraction 0.005 in the lipid and that this impurity is insoluble in the gel phase of the lipid (Sturtevant, 1982). We believe that all the lipids studied in this report are probably considerably better than 99.5 mol % pure, but this is difficult to prove.

Electron Microscopy. Samples of compound I suspended in doubly deionized water were examined by negative-staining electron microscopy before and after sonication (Figure 4). The samples were examined on copper grids (400 mesh) coated with carbon and glow discharged immediately before use. Samples were stained with 1.0% uranyl formate in doubly deionized water and examined in a Philips EM 300 electron microscope at an accelerating voltage of 80 kV.

Results and Discussion

No significant differences in calorimetric scans of I, V, and VI were found between samples run in buffer or in doubly deionized water. For I and VI the shapes of the curves of C vs. T were independent of scan rate in the range 0.02–0.23 K min^{-1}. The resolution of the peaks was definitely poorer at scan rates of 0.5 K min^{-1} or higher, indicating that between 0.02 and 0.23 K min^{-1} there are no significant kinetic limitations. For lipids IV and V the calorimetric parameters (ΔH_{cal}, ΔH_{vH}, T_m, and C_{max}) did not vary significantly between scan rates of 0.1 and 1.0 K min^{-1}, indicating that kinetic limitations are absent in their transitions at these scan rates. In all cases the scans were identical upon rescanning either immediately after cooling or after incubation in the calorimeter at 20 °C for 12 h (I, V, and VI) or at −5 °C (IV). The DASM-1M calorimeter used in this study does not scan in the cooling mode so that hysteresis effects could not be examined. The curves of C vs. T for I, V, and VI can be resolved into two or more two-state component curves. Although this analysis is convenient for the purpose of describing our observations, it does not neccessarily give a unique fit. However,

Table I: Calorimetric Parameters[a] for the Phase Transitions of Compounds I, V, and VI Observed at a Scan Rate of 0.1 K min^{-1} and Compound IV Observed at a Scan Rate of 0.5 K min^{-1}

compound	curve	$T_{1/2}$ (°C)	ΔH_{cal} (kcal mol^{-1})	ΔH_{vH} (kcal mol^{-1})	C_{max} (kcal K^{-1} mol^{-1})
I	1	39.8	4.92	140	1.0
(MLV's)	2	44.4	7.30	220	2.0
	3	46.5	4.40	700	4.0
	4	47.3	5.53	1130	7.4
	5	47.75	5.75	2040	14.0
I	1	37.0	6.2	150	1.8
(SUV's)	2	42.5	2.8	520	2.6
	3	47.5	11.5	157	3.2
	4	50.8	1.6	346	0.85
IV	1	5.0	2.4	105	0.43
(MLV's)	2	7.0	1.7	164.5	0.48
V	1	50.9	4.0	112	0.6
(MLV's)	2	55.9	2.6	427	1.6
	3	57.4	7.7	481	5.5
VI	1	51.7	1.30	295	0.5
(MLV's)	2	52.85	3.87	1160	5.3

[a] The uncertainties in the calorimetric parameters at a scan rate of 0.1 K min^{-1} are ±0.03 ($T_{1/2}$), ±0.08–0.15 (ΔH_{cal}), ±5–10 (ΔH_{vH}), and ±0.05–0.2 (C_{max}) and at a scan rate of 0.5 K min^{-1} are ±0.1 ($T_{1/2}$), ±0.12–0.30 (ΔH_{cal}), ±10–20 (ΔH_{vH}), and ±0.05–0.1 (C_{max}). At least six determinations were conducted for each compound.

the occurrence of clear inflections in the curves of C vs. T of these lipids gives added confidence that such curve fitting is a valid interpretation.

Curves of C vs. T for MLV's of compound I can be resolved into five two-state component curves (Figure 2). The values of $T_{1/2}$ for the component curves increase from 39.8 to 47.8 °C (Table I), and in going from curve 1 to curve 5, the differences in $T_{1/2}$ are in the ratios of approximately 8:4:2:1. The $T_{1/2}$ for curve 5, 47.8 °C, compares with 43.9 °C for the C_{18}:C_{16} diacylphosphatidylcholine (Chen & Sturtevant, 1981), and 49 °C for the C_{18}:C_{16} dialkylphosphatidlcholine (Bittman et al., 1981); i.e., the transition temperatures are in the order dialkyl > 1-alkyl-2-(acylamino)-2-deoxy > diacyl. Previous investigations have shown that for phosphatidylcholines the order in transition temperatures is dialkyl > diacyl > 1-alkyl-2-acyl (Boggs et al., 1981). The value of ΔH_{cal} for curve 5 (5.75 kcal mol^{-1}) is significantly lower than the corresponding values for the diacyl (7.26 kcal mol^{-1}; Chen & Sturtevant, 1981) or dialkyl (9.2 kcal mol^{-1}; Bittman et al., 1981) compounds. The total calorimetric enthalpy for compound I is 27.9 kcal mol^{-1}, which is more than 3 times the value found for the saturated 1,2-diacyl- or 1,2-dialkylphosphatidylcholines with 18-carbon chain length. The only known compounds which give comparable values for ΔH^t_{cal} are certain galactocerebrosides, e.g., *N*-palmitoylgalactosphinogosine (17.5 kcal mol^{-1}; Ruocco et al., 1983), metal ion salts of cardiolipins (24.2–30.5 kcal mol^{-1} depending on the nature of the metal ion; Rainer et al., 1979), and sodium or magnesium salts of *sn*-3,3-phosphatidyldiacylglycerols (22.2 and 23.2 kcal mol^{-1}, respectively; Rainer et al., 1979). In going from curve 1 to curve 5 there is an increase in cooperativity as measured by the ratio ΔH_{vH}:ΔH_{cal}. Subsequent to curve 2 there is an abrupt change in this ratio, from a value of about 30 for the first two curves to values of 160, 200, and 350 for curves 3, 4, and 5 respectively (i.e., approximate ratios of 1:1:5:7:12). The values of C_{max} for component curves 1–5 increase approximately in the ratios 1:2:4:7:14.

Incubation of compound I at 20 °C for 24 h after the first scan did not significantly alter the calorimetric parameters. However, an 8-day incubation under 1 atm of nitrogen at 1

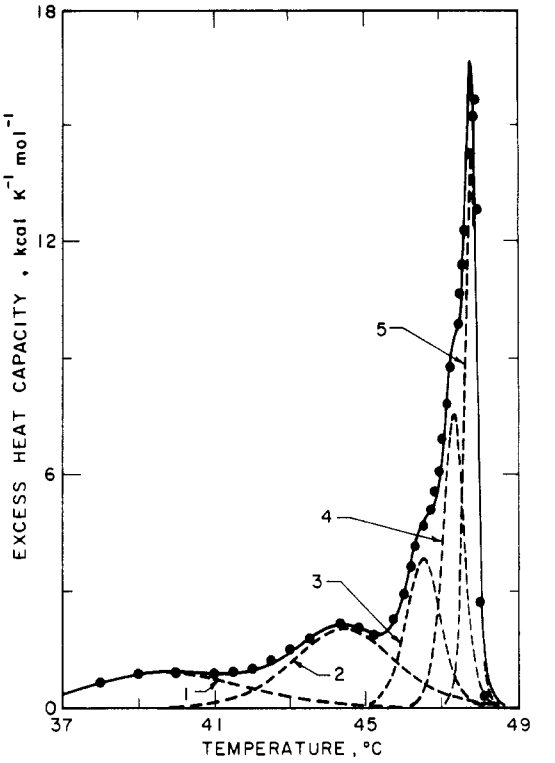

FIGURE 2: Excess heat capacity as a function of temperature (scan rate 0.1 K min^{-1}) for MLV's of compound I: (●) experimentally observed values of excess heat capacity; (- - -) component two-state transition curves obtained by computer analysis; (—) the sum of the component curves.

°C produced a different curve of C vs. T, consisting of the same number of component curves but with the $T_{1/2}$'s for all the curves raised by about 5.5 °C. A rescan of the sample after cooling and heating 4 times in the calorimeter to a temperature 5 °C above T_m gave a curve of C vs. T characterized by the same calorimetric parameters as observed prior to the low-temperature incubation. The value of ΔH^t_{cal} for the four scans was unaffected, within experimental error, by the low-temperature incubation. After incubation for 8 days at 1 °C no transition between 0 and 30 °C was observed, indicating either that compound I does not exhibit a transition similar to the subtransition observed with diacylphosphatidylcholines (Chen et al., 1980) or that the incubation conditions, time, temperature, and concentration of lipid, were not appropriate for the formation of this phase.

SUV's of compound I (Figures 3 and 4) show the calorimetric properties given in Table I. The temperature range of the curve of C vs. T is about 17 °C which is similar to that of the curve for unsonicated material, although the temperature range is shifted to higher temperatures. Samples of SUV's gave the same calorimetric curve after cooling from 2 °C above T_m to 25 °C and rescanning immediately, indicating that fusion had not occurred. However, in the present study no experiments were conducted to find under which conditions fusion of these SUV's does occur. The C_{max} for SUV's is reduced by a factor of 6 and the ΔH^t_{cal} (22.1 kcal mol^{-1}) is reduced by 20% compared to that of unsonicated suspensions. The decrease in ΔH^t_{cal} may be due to poorer packing of the phospholipid and a greater number of gauche rotamers in SUV's than in MLVs (Carey, 1982).

That the complex transition behavior of I is an intrinsic property of the lipid and is not due to metastable states, incomplete initial hydration, impurities, degradation products formed during vesicle preparation or during scanning, or vesicle inhomogeneity is clearly shown by the following observations.

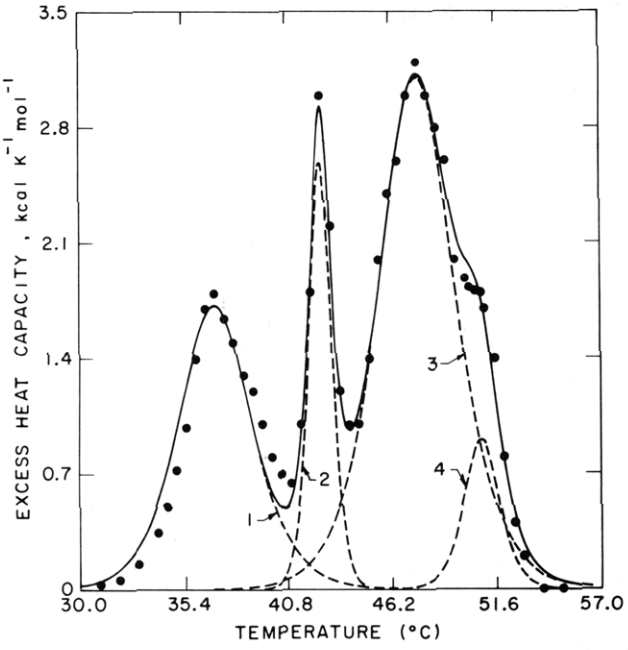

FIGURE 3: Excess heat capacity as a function of temperature (scan rate 0.1 K min^{-1}) for SUV's of compound I. The symbols are the same as in Figure 2.

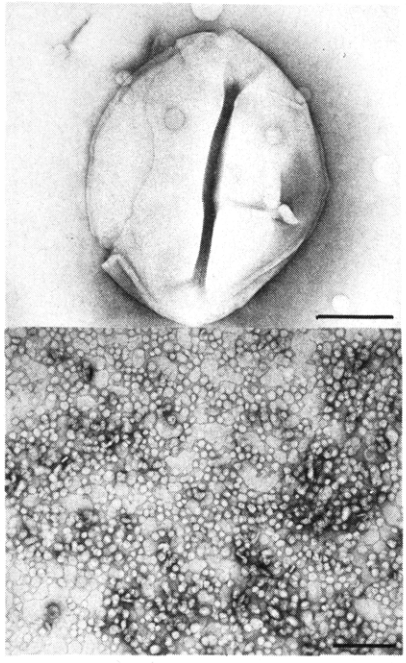

FIGURE 4: Electron micrographs of MLV's (top) and SUV's (bottom) of compound I. The bars represent 2500 (top) and 4200 Å (bottom).

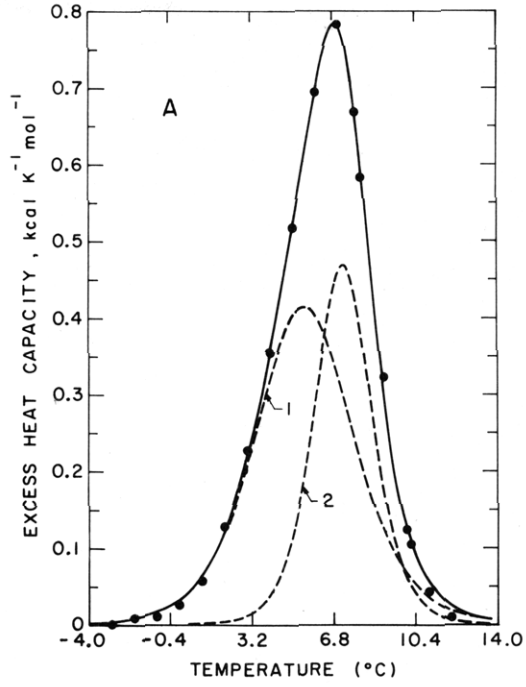

FIGURE 5: Excess heat capacity as a function of temperature (scan rate 0.5 K min^{-1}) for MLV's of compound IV. The symbols are the same as in Figure 2.

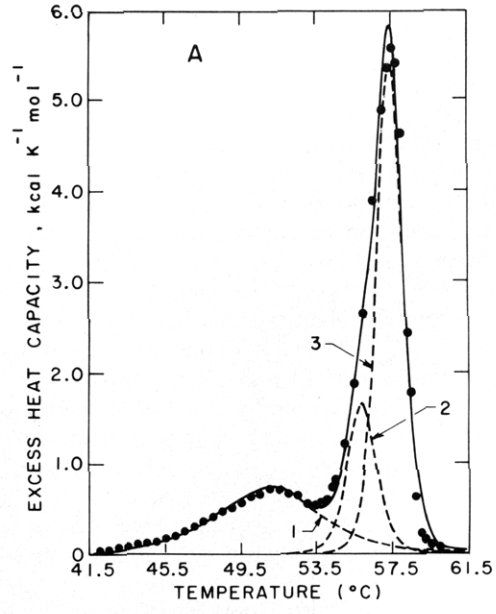

FIGURE 6: Excess heat capacity as a function of temperature (scan rate 0.1 K min^{-1}) for MLV's of compound V. The symbols are the same as in Figure 2.

The scans are fully reversible; negative staining electron microscopy shows insignificant amounts of SUV's and MLV's before and after sonication, respectively; centrifugation of MLV samples at 10^5g for 1 h followed by DSC examination of the resuspended pellet gives the same C vs. T curve as the original MLV preparation, whereas a scan of the supernatant gives no significant deviation from scans of H_2O vs. H_2O or buffer vs. buffer, and the calorimetric scans were the same before and after preparative TLC and/or recrystallization from chloroform/acetone mixtures (1:40 v/v) or from ethanol.

Compounds II and III did not exhibit any phase transitions in the temperature range −10 to 60 °C, a result which is not surprising since the ability of diacylphosphatidylcholines to form stable bilayers decreases or disappears below a chain length of 12-carbon atoms (Mabrey-Gaud, 1981). It is probable that these two phospholipids exist in aqueous suspension as micelles rather than bilayers.

Lipids IV and V gave the experimental curves of C vs. T shown in Figures 5 and 6. These thermograms can be resolved into two-state component curves, two for compound IV and three for V, with the calorimetric parameters given in Table I. The asymmetry of the thermogram for compound IV shows that a minimum of two two-state curves is required for an adequate fit.

Compound IV shows only two transitions (Figure 7; Table I). $T_{1/2}$ for curve 1 is 0.4 °C higher and that for curve 2 is 2.1 °C lower than the T_m's for the pretransition and gel to liquid-crystalline transitions of 1,2-distearoylphosphatidyl-

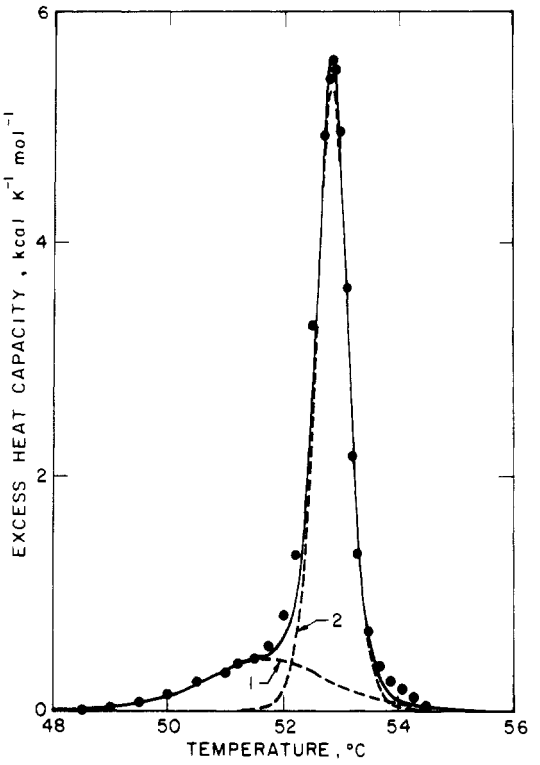

FIGURE 7: Excess heat capacity as a function of temperature (scan rate 0.1 K min^{-1}) for MLV's of compound VI. The symbols are the same as in Figure 2.

choline, respectively. However, the C_{max} and ΔH_{cal} of the gel to liquid-crystalline transition of distearoylphosphatidylcholine are higher by 100 and 200%, respectively, than the corresponding parameters for compound VI using the same scan rates (B. Z. Chowdhry et al., unpublished observations). The phase transition temperature of phosphatidylcholines in which the C-2 ester group has been replaced by the carbamoyloxy function [–NH–C(=O)–O–] have been obtained by using the fluorescent probe 8-anilinonaphthalene-1-sulfonate (Gupta et al., 1981). A T_m of 52 °C was obtained for 1-palmitoyl-2-[(heptadecanoylcarbamoyl)oxy]phosphatidylcholine.

We are unable to account for the very complex transition curve displayed by compound I. Comparison of the structure of I with that of VI indicates that much of the complex behavior of I results from the substitution of an ether linkage for an ester linkage. No such behavior has been reported to date for any other phospholipid, whether of like or mixed chain composition.

If one attempts to invoke increased hydrogen bonding due to the presence of the amide group and the possible cis–trans isomerism of this group, one is confronted with the difficulty that the presence of the amide group in compound VI leads only to relatively minor changes in transition behavior compared with 1,2-distearoylphosphatidylcholine. The unique thermotropic properties exhibited by I might result from a more hydrophobic microenvironment created by the presence of the alkoxy group near the polar part of the molecule, which could change the hydration properties of the phospholipid compared to those of compound VI, with the result that some of the component transitions of I might arise from cooperative changes in the hydration state of the phospholipid. The possibility that five distinct phases in the classical thermodynamic sense are the cause of the curve for compound I is ruled out by the Gibbs phase rule.

We propose that in the light of the results obtained with other phospholipids (Mabrey-Gaud, 1981), the final component transition in I and IV–VI represents the chain melting transitions of these compounds. The question arises as to which of the component transitions, if any, is a pretransition. The first transition components of lipids V and VI have similar calorimetric properties to the pretransitions of saturated diacylphosphatidylcholines (Mabrey & Sturtevant, 1978). It has been proposed that the pretransition in saturated diacylphosphatidylcholines may result either in part or in whole from changes in long axis molecular rotation (Scott & Coe, 1983). It may therefore be worth measuring this property as a function of temperature by nuclear magnetic resonance (Blume et al., 1982) for the lipids examined in this study. Examination of the effect upon calorimetric properties of changes in chain length and addition of small amounts of cholesterol (Mabrey et al., 1978) might also help to identify the pretransitions.

Acknowledgments

We thank Douglas Keene of the Departments of Biology and of Molecular Biophysics and Biochemistry of Yale University for the electron microscopy studies.

Registry No. I, 89044-07-5; II, 89044-08-6; III, 89044-09-7; IV, 89044-10-0; V, 89044-11-1; VI, 89044-12-2.

References

Albon, N., & Sturtevant, J. M. (1978) *Proc. Natl. Acad. Sci. U.S.A. 75*, 2258–2260.

Bittman, R., Clejan, S., Jain, M. K., Deroo, P. W., & Rosenthal, A. F. (1981) *Biochemistry 20*, 2790–2795.

Blank, M. L., Snyder, F., Byers, L. W., Brooks, B., & Muirhead, E. E. (1979) *Biochem. Biophys. Res. Commun. 90*, 1194–1200.

Blank, M. L., Lee, T. C., Fitzgerald, V., & Snyder, F. (1981) *J. Biol. Chem. 256*, 175–178.

Blume, A. (1976) Ph.D. Thesis, Freiburg University, West Germany.

Blume, A., Rice, D. M., Wittebort, R. J., & Griffin, R. G. (1982) *Biochemistry 21*, 6220–6230.

Boggs, J. M., Stamp, D., Hughes, D. W., & Deber, C. M. (1981) *Biochemistry 20*, 5728–5735.

Bonsen, P. O. M., DeHaas, G. H., Pieterson, W. A., & Van Deenan, L. L. M. (1972) *Biochim. Biophys. Acta 270*, 364–382.

Carey, P. R. (1982) in *Biochemical Applications of Raman and Resonance Raman Spectroscopies*, p 222, Academic Press, New York and London.

Chandrakumar, N. S., & Hajdu, J. (1982) *Tetrahedron Lett. 23*, 1043–1046.

Chandrakumar, N. S., & Hajdu, J. (1983) *J. Org. Chem. 48*, 1197–1202.

Chen, S. C., & Sturtevant, J. M. (1981) *Biochemistry 20*, 713–718.

Chen, S. C., Sturtevant, J. M., & Gaffney, B. (1980) *Proc. Natl. Acad. Sci. U.S.A. 77*, 5060–5063.

Dittmer, J. C., & Lester, R. L. (1964) *J. Lipid Res. 5*, 126–127.

Dittmer, J. C., & Wells, M. A. (1969) *Methods Enzymol. 14*, 482–127.

Goldfine, H., Johnston, N. C., & Phillips, M. C. (1981) *Biochemistry 20*, 2908–2916.

Gupta, C. M., & Bali, A. (1981) *Biochim. Biophys. Acta 663*, 506–515.

Harlos, K., Stumpel, J., & Eibl, H. (1979) *Biochim. Biophys. Acta 555*, 409–416.

Honma, Y., Kasukabe, T., Hozumi, M., Tsushima, S., & Nomura, H. (1981) *Cancer Res. 41*, 3211–3216.

Howard, B. V., Morris, H. P., & Bailey, J. M. (1972) *Cancer Res. 32*, 1523–1538.
Kates, M. (1978) *Prog. Chem. Fats Other Lipids 15*, 301–342.
Lee, T. C., & Fitzgerald, V. (1980) *Biochim. Biophys. Acta 598*, 189–192.
Mabrey-Gaud, S. (1981) in *Liposomes from Physical Structure to Therapeutic Applications* (Knight, C. G., Ed.) p 75, New York Press, New York.
Mabrey, S., & Sturtevant, J. M. (1978) *Methods Membr. Biol. 9*, 237–274.
Mabrey, S., Mateo, P. L., & Sturtevant, J. M. (1978) *Biochemistry 17*, 2464–2468.
Privalov, P. L., Plotnikov, V. V., & Filiminov, V. V. (1975) *J. Chem. Thermodyn. 7*, 41–47.
Rainer, S., Jain, M. K., Ramirez, F., Ivannou, P. V., Marecek, J. F., & Wagner, R. (1979) *Biochim. Biophys. Acta 558*, 187–198.
Ruocco, M. J., Shipley, G. G., & Oldfield, E. (1983) *Biophys. J. 43*, 91–102.
Schwarz, F. T., & Paltauf, F. (1977) *Biochemistry 16*, 4335–4339.
Scott, H. L. & Coe, T. J. (1983) *Biophys. J. 42*, 219–224.
Stewart, J. C. M. (1980) *Anal. Biochem. 104*, 10–14.
Sturtevant, J. M. (1982) *Proc. Natl. Acad. Sci. U.S.A. 79*, 3963–3967.
Sunder, S., Bernstein, H. J., & Paltauf, F. (1978) *Chem. Phys. Lipids 22*, 279–283.
Turcotte, J. G., Sacco, A. M., Steim, J. M., Tabak, S. A., & Notter, R. H. (1977) *Biochim. Biophys. Acta 488*, 235–248.
Vaughan, D. J., & Keough, K. M. (1974) *FEBS Lett. 47*, 158–161.
Weber, W., & Richter, I. (1982) *Biochim. Biophys. Acta 711*, 197–207.

Absorbance and Fluorescence Stopped-Flow Kinetics of *Rhus* Laccase and the Catalytic Reaction Sequence†

Finn B. Hansen, Robert W. Noble, and Murray J. Ettinger*

ABSTRACT: Anaerobic reduction of *Rhus* laccase causes a 1.76-fold increase in protein fluorescence [Goldberg, M., & Pecht, I. (1974) *Proc. Natl. Acad. Sci. U.S.A. 71*, 4684]. Parallel stopped-flow kinetic absorbance and fluorescence measurements were made to determine with which reduction step(s) the fluorescence changes were associated. Anaerobic reduction data obtained at pH 6.0, 7.4, and 8.5 with and without fluoride showed that fluorescence increases are either slower than (e.g., pH 6.0, 0.25 mM ascorbate) or faster than [e.g., pH 6.0, 0.1 mM $Ru(NH_3)_6^{2+}$] net type 1 Cu(II) reduction. Fluorescence increases are usually slower than type 3 reduction. However, type 3 reduction and fluorescence enhancement profiles are congruent in the presence of fluoride or at pH 8.5; the fluorescence changes are never faster than type 3 reduction. The forms of the fluorescence kinetic profiles invariably are similar to the type 3 reduction profiles and not the type 1. The oxidation of reduced copper sites by O_2 and the associated fluorescence decrease occur with the same rate constant. Satisfactory simulations are only obtained by assuming that two fluorescence changes occur which are associated with two separate reduction steps. The data are consistent with a first fluorescence increase occurring upon type 3 reduction and a second with the *final* type 1 Cu(II) reduction. This suggests that a change in protein conformation occurs when the type 3 site is reduced which in turn makes fluorescence sensitive to the redox state of the type 1 copper. pH-jump experiments indicate that the active and inactive forms evident at pH 7.4 and 8.5 [Andréasson, L.-E., & Reinhammar, B. (1976) *Biochim. Biophys. Acta 445*, 579] are not in equilibrium in the fully oxidized enzyme.

Laccases catalyze the oxidation of a variety of reductants and use oxygen as the sole electron acceptor to form water. The enzymes isolated from the Japanese lacquer tree *Rhus vernicifera* and the fungus *Polyporus versicolor* are the most extensively characterized to date (Malmström et al., 1975; Holwerda et al., 1976; Reinhammar & Malmström, 1981; Farver & Pecht, 1981). Four tightly bound Cu(II) atoms are essential for catalytic activity in both laccases. These are distinguished by their spectroscopic parameters into three types. Extensive transient kinetic studies indicate that both type 1 Cu(I) and type 2 Cu(I) are required for the reduction of the type 3 Cu(II) pair (Andréasson et al., 1973b; Brändén & Reinhammar, 1975; Pecht & Farraggi, 1971; Pecht, 1979; Andréasson & Reinhammar, 1976, 1979; Dawson et al., 1972; Holwerda & Gray, 1974, 1975; Wherland et al., 1975; Holwerda et al., 1978). Current kinetic schemes propose that type 1 Cu(II) reduction precedes type 2 Cu(II) reduction before type 3 reduction occurs via intramolecular electron transfer from the type 1 and type 2 sites (Andréasson & Reinhammar, 1976, 1979; Malmström, 1982). The type 3 pair acts as a cooperative two-electron acceptor, at least under some conditions (Malkin et al., 1969; Reinhammar & Vänngård, 1971; Reinhammar, 1972; Farver et al., 1978). An added complexity in the kinetics of anaerobic reduction of *Rhus* laccase is that two forms of the oxidized enzyme in slow exchange have been postulated to account for biphasic reduction profiles at pH 7.4 under rapid reducing conditions (Holwerda & Gray, 1974; Andréasson & Reinhammar, 1976, 1979).

Reoxidations of types 1 and 3 Cu(I) by O_2 are very rapid (Andréasson et al., 1973a, 1976), while reoxidation of type 2 Cu(I) by O_2 is much more sluggish (Andréasson et al., 1973a; Brändén & Deinum, 1978). The reduced type 3 site

† From the Departments of Biochemistry and Medicine, State University of New York at Buffalo, Buffalo, New York 14214. *Received May 19, 1983; revised manuscript received November 15, 1983.* This work was supported by National Science Foundation Grant BMS 73-01248A01 and by funds to the Bioinorganic Graduate Group from the Graduate School of the State University of New York at Buffalo. F.B.H. received support from the Graduate School, the Nato Science Fellowship Fund, and the Danish Carlsberg Foundation. R.W.N. received research support from the Veterans Administration.

* Address correspondence to this author at the Department of Biochemistry, State University of New York at Buffalo.

0006-2960/84/0423-2049$01.50/0